REVIEW

Methods for probing water at the nanoscale

Jason Knowles Holt

Abstract A review of selected experimental and modeling techniques that have been applied to study water structure and dynamics will be presented. Many of these techniques provide atomic and molecular level detail about water and are thus relevant to nanofluidics. Given the wealth of simulations and recent experimental reports on water confinement in carbon nanotubes, many of the examples provided will focus on this unique system. Finally, some perspectives on the picture of water that has emerged from these various studies will be offered.

Keywords Carbon nanotubes · Nanofluidics · Water structure · Flow simulations

1 Introduction

Nanofluidics involves the study of fluid flow on length scales commensurate with molecules, and, as such, opens the door to studying a host of interesting physical phenomena and enables many unique applications. As pointed out in an excellent earlier review (Eijkel and van den Berg 2005), nanofluidics is not a new discipline, but its recent emergence as such may reflect the explosion of interest in nanomaterials and in the tools capable of characterizing them. Examples of fluids confined at the nanometer scale are found in nature, in fields as diverse as biology (e.g., aquaporin water channels in our cells; Agre 2004) and geology (e.g., hydrocarbon diffusion through rocks; Leythaeuser et al. 1980)

J. K. Holt (✉)
Chemical Sciences Division, L-231, Lawrence Livermore
National Laboratory, Livermore, CA 94550, USA
e-mail: holt14@llnl.gov; jasonkholt@yahoo.com

Recently, researchers have managed to produce nanomaterials and devices incorporating them that mimic, to some degree, the function of natural systems. Carbon nanotubes (CNTs), for example, are synthetic channels with a size range comparable to many biological channels. Also, they possess hydrophobic surfaces and can be functionalized (Chen et al. 1998; Dyke and Tour 2004). These biomimetic properties initially motivated theorists to model the fluid transport characteristics of CNTs using molecular simulations, and the predicted flow rates were comparable and in some cases larger than those seen in aquaporin channels (Hummer et al. 2001; Kalra et al. 2003). Researchers have recently succeeded in producing CNT membranes, in an effort to exploit these unique transport characteristics on the macroscale (Hinds et al. 2004; Holt et al. 2004; Majumder et al. 2005; Holt et al. 2006). In agreement with the molecular simulations, significant enhancements in transport were observed, with measured water flow rates many orders of magnitude higher than the predictions of continuum hydrodynamics. An open question, however, is whether the flow enhancement can be attributed to a molecular ordering phenomenon, as the simulations have suggested. For comparison, Fig. 1 illustrates a natural aquaporin water channel and a single wall carbon nanotube (SWCNT), where the combination of the pore structure and functionality in the former and the confinement and hydrophobicity of the latter contribute to water structural ordering.

While one may gain insights into fluid properties through macroscopic flow measurements, it is clear that below a certain size regime, it is necessary to consider the granularity of a fluid. In nanofluidics, the detailed interactions of molecules with one another and with the surrounding surfaces dominate the fluid properties. Therefore, macroscopic properties such as viscosity and
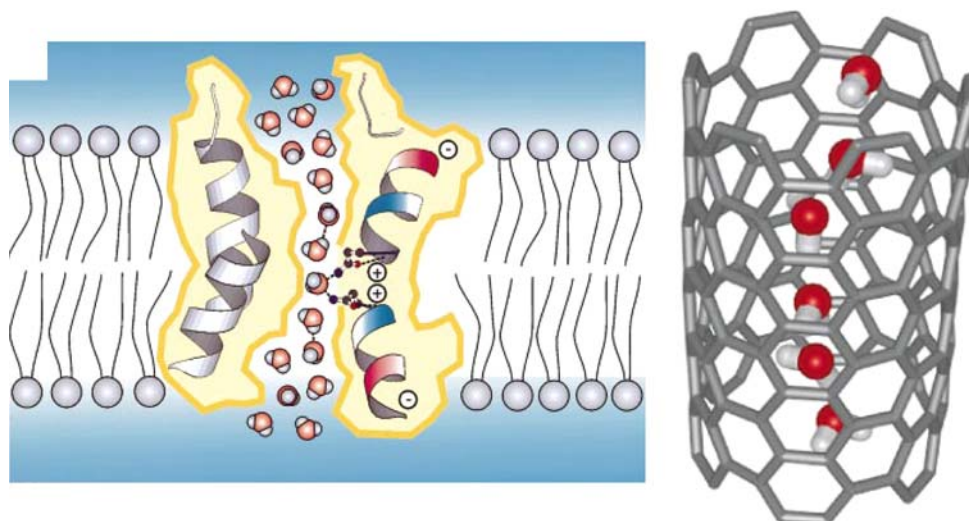
Fig. 1 *Left*: illustration of a natural aquaporin water channel, regarded as the "plumbing systems for cells". Water is confined in the 2 nm restriction of this hourglass structure, adopting a single file structure. Water also experiences interactions with pore functionalities, preventing the formation of hydrogen bonds between water molecules, and thus blocking proton transport, which is the key to the biological function of this protein. Reprinted with permission from Murata et al. (2000). *Right*: illustration of water ordering phenomenon within a single wall CNT, attributed in part to confinement effects and the hydrophobicity of the surface. Reprinted with permission from Hummer et al. (2001)

density may not provide an adequate description of fluid behavior. To further illustrate this point, consider bacteriorhodopsins, which are trans-membrane proteins that function as proton pumps (Landau and Rosenbusch 1996). The size and surface properties of these proteins are such that they impose ordering of water molecules within the channel and, in contrast to aquaporins, form so-called "water wires" that enable hopping of protons through the Grotthus mechanism (Agmon 1995). In addition to the interaction of water molecules with one another at the nanoscale, their participation as a ligand in ion coordination is also biologically significant. Highlighting this point is the potassium ion channel, a key component of the electrical signaling process in organisms, which permits the selective transport of potassium ions while blocking the transport of other ions such as sodium (Jessel 2000). The basis for this selective behavior is the specific functionalization of the channel, i.e., functional groups within the channel that are positioned to mimic the hydrated state of the potassium ion in solution. This allows the channel to strip the hydrated potassium ion of its water molecules without an energy penalty, providing a type of catalyzed ion transport. Ions slightly different in size such as sodium do not precisely fit within the channel, and thus cannot be dehydrated to facilitate transport (Doyle et al. 1998; Agre and MacKinnon 2003). Figure 2 illustrates the potassium ion channel and how it achieves this exquisite selectivity. It is worth mentioning that the key insights into the function of these molecular machines were enabled by the availability of techniques capable of
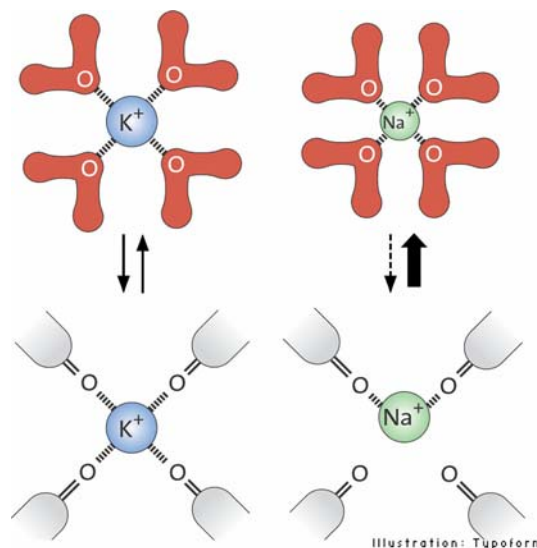

Fig. 2 Potassium ion channels permit the transport of potassium, while blocking the transport of sodium ions. The root of this selectivity lies in the positioning of oxygen functionalities within the filter region that precisely fit a hydrated potassium ion, but do not fit a hydrated sodium ion. Reprinted with permission from Agre and MacKinnon (2003), ©The Nobel Foundation

probing the detailed atomic structure and dynamics of these systems, such as high resolution X-ray crystallography and molecular modeling. The availability of such techniques and the resulting understanding of this key biological mechanism garnered MacKinnon a share of the 2003 Nobel Prize in Chemistry.

In nanofluidics, there is often a focus on the characterization of forces, such as those resulting from interactions between solvent molecules and surface mediated interactions, since these forces govern a host of different fluid phenomena (Eijkel and van den Berg 2005). The experimental techniques that have been applied to study these forces include the surface forces apparatus and, more recently, the atomic force microscope (Koumoutsakos et al. 2004). Given the atomic/molecular origin of these forces, a detailed knowledge of water structure and dynamics at the nanoscale is clearly beneficial to the discipline of nanofluidics. As such, there is a need for techniques capable of probing water on these length scales, particularly as researchers attempt to build nanofluidic devices that utilize some of the unique phenomena that nature has provided us.

With this rationale established, this review will focus in part on the various experimental techniques that are applied to study the structure and dynamics of water on the nanoscale. While the study of confined, hydrated ions is also interesting, and is relevant to a number of practical applications, water is a challenging enough topic itself to cover in any breadth. A central issue in studying water concerns the nature of the hydrogen bonding (HB) network in the liquid state, which explains a number of its unique bulk properties (e.g., density maximum upon cooling from room temperature, with a rapid density decrease below 277 K; Ludwig 2001) as well as the novel properties predicted at the nanoscale. A number of techniques will be presented that are used to study this HB network, both directly and indirectly. Many of the examples presented focus on CNTs, given that they are widely regarded as the prototypical nanomaterial, as well as an idealized nanofluidic channel. A review of this kind would not be complete without a discussion of the application of modeling, both molecular and continuum mechanical, to the study of water in bulk and under confinement. While the relevant literature, particularly on molecular modeling of water, is too vast to cover in detail, an attempt will be made to provide some perspective on what has been learned from such simulations and to provide recent examples of their application to nanofluidics. The intent here is not to provide an exhaustive review of all possible methods to address the problem, but to present an overview of selected techniques, their strengths and limitations, and what insights they have provided into water structure and dynamics. The interested reader is referred to a comprehensive review of computational nanoscale fluid mechanics by Koumoutsakos et al. (2004)

2 Experimental techniques

Before launching into a discussion of specific techniques, it is worth noting the general view of bulk water structure and dynamics that has emerged from decades worth of studies. As Stillinger (1980) summarizes in his review on the state of knowledge of water 25 years ago (a picture that has in a general sense remained intact), water is envisioned as a random or disordered network of molecules connected by hydrogen bonds that undergo rapid fluctuation. More specifically, the time scales for these hydrogen bond breaking and reforming steps are extremely fast, spanning the range from femto to picoseconds (Tokmakoff 2007). As might be expected, there is no single technique that can provide both a complete picture of water's molecular structure and its rapid dynamics. Thus, in considering the type of technique to use in probing water, one must ask whether they are most concerned with an accurate determination of structure or whether the dynamics are more important. X-ray and neutron scattering provide structural information, albeit at the expense of dynamical information. On the other hand, there are a number of techniques (e.g., time-resolved infrared spectroscopy) that provide key insights into water dynamics on time scales commensurate with its fluctuation and reorganization, although they may lack the structural detail that the scattering techniques provide.

2.1 Structural techniques

Scattering techniques have been the workhorses for the determination of water structure and thus some of the results of these studies will be highlighted. There have been also recent X-ray absorption and X-ray Raman scattering studies that appear to provide a picture of water that differs markedly from the conventional view. This controversy and current views on water structure will be highlighted.

2.1.1 X-ray, neutron diffraction and scattering

Historically, the determination of water structure has been carried out using X-ray (Morgan and Warren 1938; Karnicky and Pings 1976) and neutron scattering techniques (Page 1972; Narten et al. 1982). Although the terms diffraction and scattering are often used interchangeably, diffraction techniques are usually used in the context of atomic structure determination in crystalline materials with long-range order, whereas scattering techniques are used for determining atomic structure in non-crystalline materials (e.g., liquid water). X-rays and neutrons interact with materials in a fundamentally different manner, and thus provide different probes of water structure. X-rays are scattered by the electron clouds around atoms and molecules, and thus for the case of water, a greater degree of scattering is offered by the oxygen atoms than the hydrogen atoms (Head-Gordon and Hura 2002). By contrast, neutrons interact with atomic nuclei, an attribute that
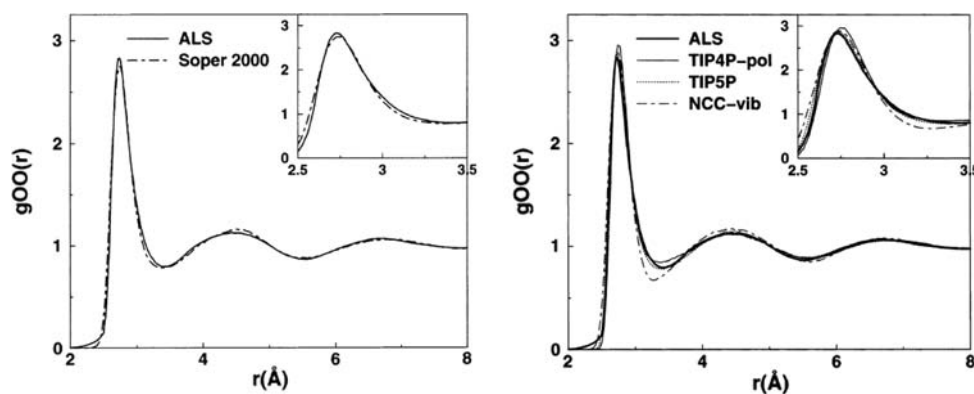
Fig. 3 *Left*: a comparison of $g_{OO}(r)$ derived from X-ray (*ALS*) and neutron scattering (Soper 2000) measurements on pure water under ambient conditions. *Right*: a comparison of $g_{OO}(r)$ derived from X-ray scattering (*ALS*) measurements and predictions of a nonpolarizable water model (*TIP5P*) and two polarizable water models (*TIP4P-pol*, *NCC-vib*). Adapted and reprinted with permission from Head-Gordon and Hura (2002)

enables a hydrogen sensitivity that is not possible with X-rays, allowing the details of hydrogen structure to be probed (Head-Gordon and Hura 2002).

One key parameter that can be extracted from X-ray scattering measurements on water is the coordination number, derived from the oxygen–oxygen radial distribution function, $g_{OO}(r)$, which is a measure of the distribution of mean interatomic distances between oxygen atoms. While this topic will be covered in greater depth in the section "Modeling techniques", it is worth noting that modeling and simulations are a key complement to these scattering measurements, as one can simulate distribution functions and use this as a test of the reliability of the empirical water models employed. Recent measurements of bulk water under ambient conditions have suggested a coordination number of 4.7 (Hura et al. 2000), suggesting that liquid water retains some of the tetrahedral structure characteristic of ice, albeit with deformations in hydrogen bonding patterns. These results indicate a higher degree of structural ordering in liquid water than that suggested by previous studies (Narten et al. 1982; Soper et al. 1997). An analysis of neutron scattering data (Soper 2000) produced results similar to those obtained by X-ray scattering, with a similar $g_{OO}(r)$, as seen in Fig. 3a. Because of the minute details of water structure that these experimental techniques provide, they serve as a crucial benchmark by which the quality of simulations can be measured. Simulations utilizing polarizable[1] (Rullmann and Vanduijnen 1988; Sprik and Klein 1988) and nonpolarizable models for water do an acceptable job of reproducing $g_{OO}(r)$, as seen in

Fig. 3b. Due to the differences in the nature of neutron interactions, information on oxygen–hydrogen ($g_{OH}(r)$) and hydrogen–hydrogen ($g_{HH}(r)$) interactions is also obtained from neutron scattering data. Mutiple experimental measurements of these distribution functions (Soper et al 1997; Soper 2000) show reproducibility. However, the same polarizable model simulations are often not as successful in reproducing these functions.

One application of these methods in nanofluidics involved neutron scattering, coupled with molecular dynamics, to study water confined within SWCNTs (Kolesnikov et al 2004). These studies were intended to test earlier predictions of one-dimensional molecular ordering within SWCNTs (Hummer et al. 2001; Kalra et al. 2003). The structure resulting from the simulations that best reproduces the experimental measurements is a two-phase system: interior water forms a fourfold coordinated ice sheet wrapped into a cylinder near the nanotube wall, as well as a one-dimensional chain of water molecules (average coordination number 1.86) along the tube axis that retains fluidity down to as low as 50 K (Fig. 4). These results are significant, given the similarities in size and surface properties between these hydrophobic CNTs and transmembrane protein channels such as aquaporins.

2.1.2 X-ray absorption spectroscopy (XAS)

XAS is a technique that enables the local structure around a specific element to be determined. Among its principle advantages, XAS is used to analyze solids and liquids nondestructively, with concentrations of the target element as low as 10 ppm. An X-ray absorption spectrum is produced when an atom absorbs an X-ray whose energy corresponds to an electron binding energy for the atom in the material. This photoelectron can scatter off surrounding atoms or in select cases the electron can be excited into

---

[1] Polarizable models are based on induced dipoles in which the electric field caused by other atoms and molecules leads to the polarization of an atom center. This polarization effect itself leads to a field that affects the neighboring atoms/molecules and their respective field. This is a way of including "many-body" effects that are not included in simpler pairwise potential models.
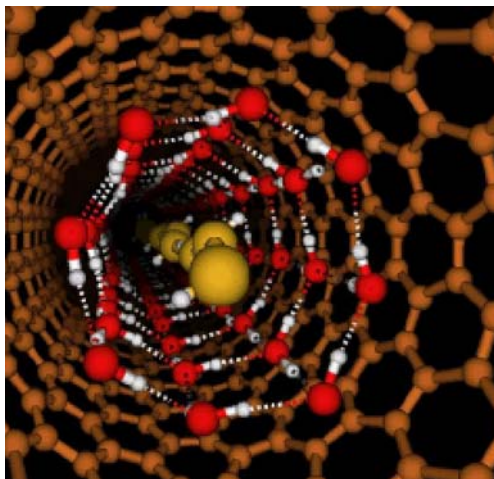
Fig. 4 Illustration of proposed water structure within a 1.4 nm diameter single wall CNT. *Red* corresponds to oxygen atoms of fourfold coordinated water molecules wrapped into a cylindrical ice sheet. *Yellow* corresponds to oxygen atoms of water molecules in a one-dimensional chain along the nanotube axis. Adapted and reprinted with permission from Kolesnikov et al. (2004)

vacant states near the valence band (Fig. 5). X-ray absorption spectra are typically divided into two regions: the X-ray absorption near edge structure (XANES), which is located at energies near the absorption edge, and the extended X-ray absorption fine structure (EXAFS), which can extend to energies of up to 1,000 eV past the absorption edge. The XANES region provides electronic structure information about the absorbing atom, such as its valence state and density of states, while the EXAFS region contains information on local atomic structure (Newville 2004). Figure 5 shows these different regions of an XAS spectrum.

XAS is also a particularly useful technique in probing ultrafast processes because of the fast time scale for X-ray absorption ($<10^{-15}$ s), allowing frozen configurations of molecules such as water to be interrogated, whose vibrational motions occur on much longer time scales (10^{-15} to 10^{-12} s). Specifically, the method can be used to obtain the instantaneous electronic structure of oxygen atoms

(examining the oxygen K-edge) in a water molecule ensemble, allowing the hydrogen bond configuration to be extracted through the use of quantum level calculations (Myneni et al. 2002). However, such experiments on liquids in the soft-X-ray regime are by no means trivial, with problems associated with the short attenuation lengths ($\sim$microns) at these X-ray energies that make transmission experiments difficult, and saturation effects that complicate fluorescence-based detection (Bergmann et al. 2002). While the focus in this review is on water, it is worth mentioning that XAS is also useful in interrogating the structure of hydrated ions. Particularly for larger ions (e.g., Br^-), whose K-edge absorption energies are relatively large, there are fewer experimental difficulties than encountered in the soft X-ray regime. XAS has been used to study the structure of Br^- under both ambient and supercritical conditions (Wallen et al. 1997), as well as within carbon nanopores (Ohkubo et al. 2002), with indications of a significant reduction in coordination number upon confinement.

Although difficult, a few XAS studies of bulk water under ambient conditions have been reported. One study (Smith et al. 2004) involved the use of a liquid microjet and the measurement of oxygen K-edge X-ray absorption by the total electron yield (TEY) method. During cooling of the water microjet in the vacuum environment, a noticeable decrease in pre-edge intensity was seen, associated with hydrogen bonds being broken on the H-donating site of the water molecules, with a simultaneous increase in post-edge intensity, associated with a symmetric ice-like configuration (see Fig. 6). The authors concluded that their data support the "standard model" for water, consisting of a random tetrahedral network with a coordination number of 4. Seemingly contrary results had earlier been reported (Myneni et al. 2002), in which significant differences in the electronic structure of liquid water versus that in solid or gaseous forms were found. Specifically, there was a noticeable increase in intensity in this pre-edge region (oxygen K-edge) relative to ice. It was found that the spectral features were dictated primarily by the first shell coordination, and three different structures were proposed:

Fig. 5 *Left*: illustration of the X-ray photoelectric effect wherein an X-ray is absorbed and a core-level electron is ejected. *Right*: XAS spectrum (absorption coefficient as a function of X-ray energy) for FeO. Adapted and reprinted with permission from Newville (2004)
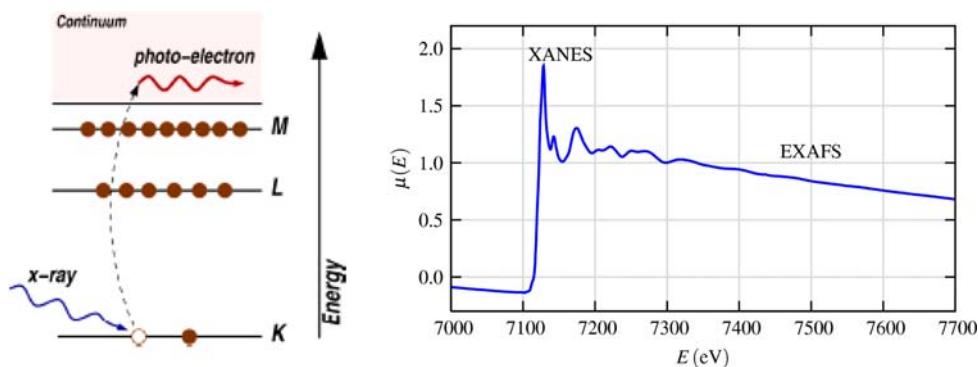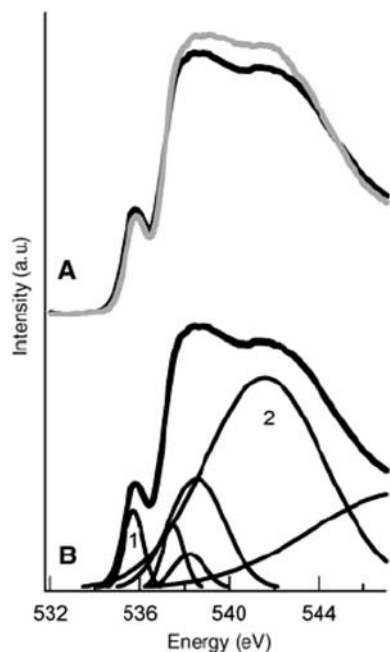
Fig. 6 Oxygen K-edge NEXAFS spectra for water at 288 K (*black*) and 254 K (*gray*) (*A*). Deconvolution of the 288 K spectrum into its Gaussian components (*B*). Bands *1* (pre-edge) and *2* (post-edge) are the only to exhibit a temperature dependence. The pre-edge region is associated with water molecules having broken or distorted hydrogen bonds on the donor side. The post-edge region is associated with water molecules having four strong and symmetric hydrogen bonds, as in ice. Reprinted with permission from Smith et al. (2004). Copyright (2004) AAAS

one symmetric (fourfold coordinated) and two asymmetric (<fourfold coordinated) hydrogen bonding structures (Fig. 7). From an analysis of the relative proportion of each structure that could accurately reproduce the spectral features, water was believed to consist primarily of one of the asymmetric structures in its first shell, with the HB being broken on the hydrogen-donating site of the molecule. Significantly, these results suggested that a large proportion
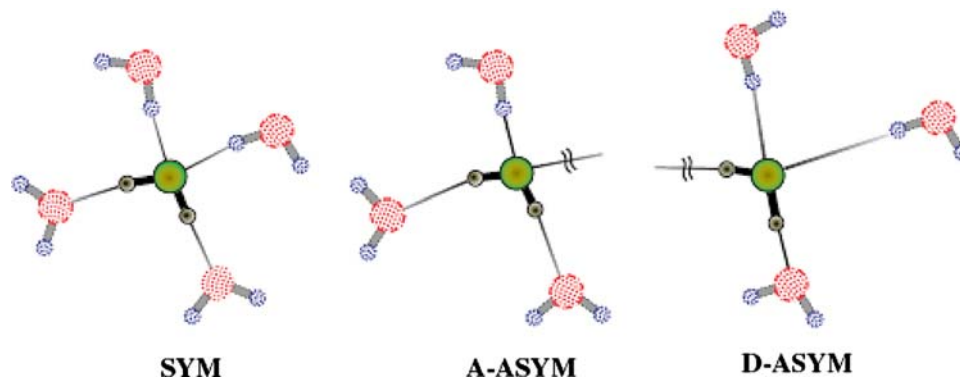
of water molecules exist in an unsaturated hydrogen bonding environment, having a coordination number as small as 2.4, contrary to the tetrahedral "standard model".

2.1.3 X-ray Raman scattering (XRS)

In contrast to XAS, which is performed at energies near electron binding energies (e.g., 284 eV for C K-edge), X-ray Raman scattering (XRS) involves higher energies (e.g., $\sim$8,400 eV; Tohji and Udagawa 1989). Specifically, XRS is the tail of the Compton band, associated with inelastic scattering via ionization of K-level electrons. Figure 8 schematically illustrates the difference between XAS and XRS processes. XRS is a technique that overcomes some of the experimental challenges associated with low Z (e.g., oxygen, carbon) EXAFS. Low Z EXAFS experiments are conventionally carried out in the soft X-ray regime, which usually necessitates vacuum conditions, placing limits on the types of samples that can be analyzed. By operation in the hard X-ray regime, XRS eliminates the need for vacuum conditions and allows greater flexibility in sample type (e.g., liquids, thick films). Tohji and Udagawa (1989) were the first to demonstrate, using graphite and diamond samples, that the information on local structure around low Z elements provided by hard X-ray XRS is identical to that provided by soft X-ray EXAFS.

A recent XRS study that is relevant to our discussions here on water structure and nanofluidics concerns the first hydration shell of a water molecule in liquid water (Wernet et al. 2004); this study also involved the use of XAS, providing complementary spectral information. Summarizing their findings, through these experimental measurements and theoretical simulations, water molecules were believed to have only two hydrogen bonds, a conclusion similar to that reached in the earlier study (Myneni et al. 2002). More specifically, however, liquid water was believed to have one

Fig. 7 Proposed first-shell coordination structures for water that dictate the XAS features at the oxygen K-edge. *SYM* corresponds to a fourfold coordinated symmetric hydrogen bonded structure. *A-ASYM* corresponds to a threefold coordinated asymmetric structure with the

broken bond on the oxygen atom, whereas *D-ASYM* has the broken bond on the hydrogen atom. Reprinted with permission from Myneni et al. (2002)
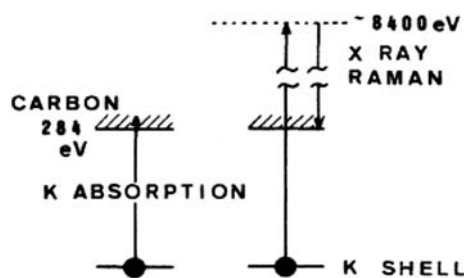
Fig. 8 Schematic of XAS using soft X-rays versus XRS, an inelastic scattering process, using hard X-rays. Reprinted with permission from Tohji and Udagawa (1989)

strong donor and one strong acceptor, and forms primarily rings or chains (Fig. 9). These results again challenge the tetrahedral "standard model" and suggest that water molecules in liquid water resemble those on the surface of ice.

2.1.4 New insights

Not surprisingly, the results discussed above have generated a great deal of controversy about water structure, as well as a spirited dialogue in the literature (Nilsson et al. 2005; Smith et al. 2005a) concerning the quality of the
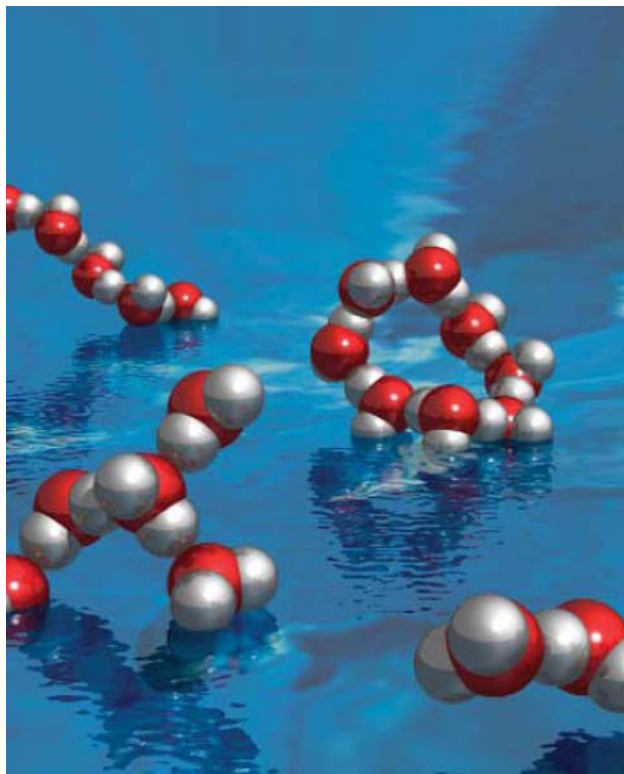

Fig. 9 Illustration of proposed ring and chain structures for water under ambient conditions, based on an analysis of XRS/XAS results (Wernet et al. 2004). These structures are more reminiscent of the surface of ice, rather than bulk water. Reprinted with permission from Zubavicus and Grunze (2004). Copyright (2004) AAAS

absorption spectra and the analysis employed to extract hydrogen bonding configurations. Thus, one might understandably ask, which picture is correct? The answer is not straightforward and requires more careful examination.

Head-Gordon and Johnson (Head-Gordon and Johnson 2006) recently reexamined the earlier XAS experiment (Wernet et al. 2004) and attempted to simulate the spectra using density functional theory and considering water clusters that span the range from fully tetrahedrally bonded to broken donor hydrogen bonds. The central question of this study was whether the asymmetry in the electron density of a water molecule was persistent throughout all local liquid water environments and did not fluctuate, as this argument was used to support the picture of water consisting of chains or rings with two hydrogen bonds per molecule. The finding of this study was that while this asymmetry is consistent with X-ray scattering data of small length scale correlations in the liquid, it is inconsistent with the longer-range correlations from which the tetrahedral network picture is derived. This result points to the need of carefully considering what each experimental technique provides: X-ray and neutron scattering provide bulk structural measurements involving static averaging over small and large length scale structures in the liquid, whereas XAS interrogates instantaneous, small length scale structures that may not be persistent throughout. Another study (Smith et al. 2005b) utilizing temperature-dependent spontaneous Raman spectroscopy also bolsters the view of liquid water as locally tetrahedral.

Thus, the picture of water structure that appears consistent with the majority of studies to date is one of tetrahedral structure, both locally and over long length scales. With the insights gained here, it will be useful to apply a similar suite of techniques to the study of the structure of confined water in model systems like CNTs, as demonstrated as possible by recent work (Kolesnikov et al. 2004).

2.2 Structural and dynamical techniques

Water structure is of course just one part of the puzzle, and there are a number of techniques capable of probing the dynamics of water, both in bulk and within confined geometries. One goal here is to establish the linkage between structure and dynamics. For example, concerning transport through nanotubes, is molecular ordering responsible for the fast flow observed? The suite of techniques to be described has the potential to answer this and other questions.

2.2.1 Time-resolved infrared spectroscopy

One technique that provides insights into the dynamics of the hydrogen bonded network of water molecules is

time-resolved infrared spectroscopy. The intramolecular OH stretching vibration of water molecules is a sensitive probe of their hydrogen bonding environment, making the technique potentially valuable for the study of confined water, in which changes in this environment can take place. One study (Fecko et al. 2003) utilized 52 fs IR pulses and examined changes in the OH stretching frequency of HOD (1% concentration) in D_2O. They report an underdamped oscillation of the hydrogen bond with a period of 170 fs at these short probing time scales. For longer time scales of hundreds of fs to ps, characteristic of previous studies (Gale et al. 1999; Yeremenko et al. 2003), vibrational dynamics are characterized by hydrogen bond breaking and reforming with the concerted motion of several water molecules, but the specific motion of hydrogen bond stretching cannot be probed on these time scales. A later study (Cowan et al. 2005) utilized a specially designed thin sample cell to enable the study of OH vibrations in pure H_2O. These changes in experimental design led to the observation of significantly faster hydrogen bond dynamics (by approximately a factor of 10) than seen in earlier studies. Specifically, the "memory" of structural correlations in water was lost within 50 fs, indicative of the efficient redistribution of energy within the hydrogen bond network (Fig. 10). These studies highlight an important point that the "picture" one forms of water depends to a large part on the time scale that is being probed, and conclusions drawn about water structure and dynamics must be viewed with this point in mind.

2.2.2 Transmission electron microscopy (TEM)

A very different technique for studying water on the nano-scale involves direct observation by TEM. Electrons, as opposed to photons of visible light, have wavelengths in the sub-nm size regime at conventional TEM accelerating voltages (100s kV), making TEM a potentially promising way to "visualize" nanofluids (Riegelman et al. 2006). The one obvious limitation that electron microscopy presents is the need for vacuum conditions. A solution to this problem is the use of electron transparent vessels for encapsulating fluids such as CNTs. Gogotsi et al. (Naguib et al. 2004; Yazicioglu et al. 2005; Mattia et al. 2007) have conducted a number of in situ TEM studies of fluids confined within CNTs, ranging in size from 1 to 100 nm. These studies utilize "hydrothermal" nanotubes (Libera and Gogotsi 2001), in which liquid inclusions are trapped inside the tubes during synthesis, or nanotubes that are filled by autoclave treatment, followed by cooling, during which water condensation occurs (Naguib et al. 2004). Using either focusing/defocusing of the electron beam or a heating stage, the trapped fluid can be heated or cooled, allowing for direct visualization of nanofluidic transport phenomena.
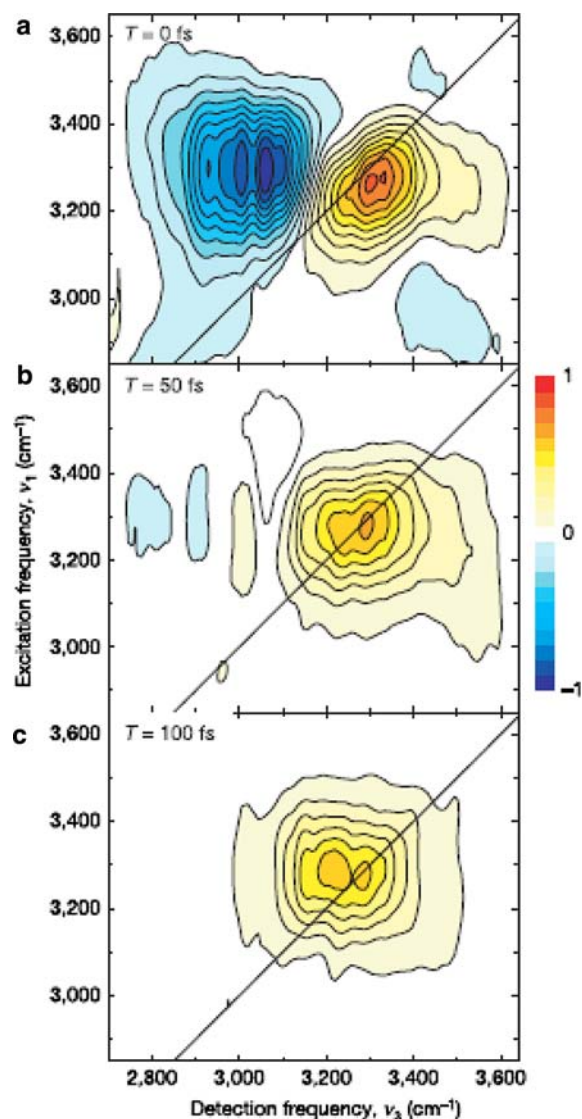

Fig. 10 Two-dimensional infrared spectra of pure liquid water for different population times (**a**, **b**, **c**). The initial inhomogeneity observed at $T = 0$ fs decays almost completely within 50 fs and is completely absent within 100 fs, illustrating a "rapid dephasing" and "loss of memory" in the system, faster than that observed with any other liquid. Reprinted with permission of Cowan et al. (2005)

Interrogating this trapped fluid inside the nanotubes, a number of interesting observations were made. During electron beam heating within a 10 nm inner diameter CNT, water was observed to undergo an apparent volume expansion (Fig. 11a, b). Using resistive heating, additional interesting phenomena were observed. Fluid evaporation occurred relatively slowly, whereas condensation occurred rapidly, suggesting elevated pressures inside the nanotubes. In 5 nm inner diameter CNTs, electron beam heating induces apparent nanobubble formation due to water evaporation (Fig. 11c, d). The time scale for this process is relatively long (~ 1 minute) compared to that expected for bulk water, suggesting the possible influence of hydroxyl

Fig. 11 Observation of dynamic fluid phenomena within water-filled multiwall CNTs. **a**, **b** Electron beam heating-induced volumetric expansion of water, along with disordering of the CNT walls. **c**, **d** Water evaporation and apparent nanobubble formation (indicated by *arrows*) within a MWCNT. The time elapsed between images (**c**) and (**d**) is approximately 1 min. Adapted and reprinted with permission from Naguib et al. (2004)
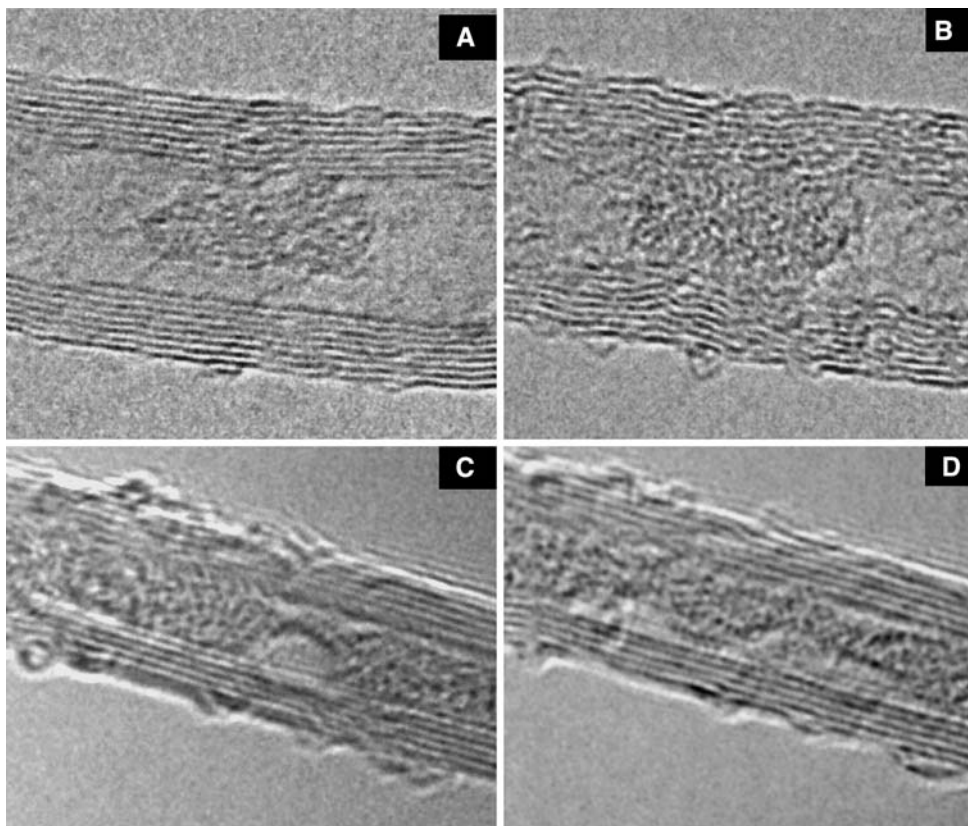
groups or other defects on the inner walls of the tube that significantly disrupt intermolecular hydrogen bonding and retard the fluidity. More detailed studies with CNTs of variable defect density would be useful for future nanofludics application development. The pristine, defect-free CNT is a simplification often used in simulation, but unlikely to be realized in practice.

Later studies have revealed well-defined, continuous menisci on nanotubes with inner diameters as small as 10 nm (Mattia et al. 2007). However, for nanotubes of 3–6 nm inner diameter, a distinct liquid/vapor interface is no longer discernable, perhaps suggesting that this defines the critical length scale at which the continuum approximation for fluid transport breaks down. Figure 12 is a TEM image of a very diffuse liquid/gas interface within a 4 nm inner diameter CNT filled by autoclave treatment. Another technique complementary to TEM that is worth mentioning is electron energy loss spectroscopy (EELS), offering chemically specific information at TEM spatial resolutions. EELS was used in conjunction with these in situ TEM measurements to identify ice confined in carbon nanotubes under cryogenic conditions (Ye et al. 2004).

On even smaller length scales (1–3 nm inner diameter; Mattia et al. 2007) these in situ measurements suggest the formation of water chains in the tube interior that adopt a double-helix structure along the tube axis, in a manner
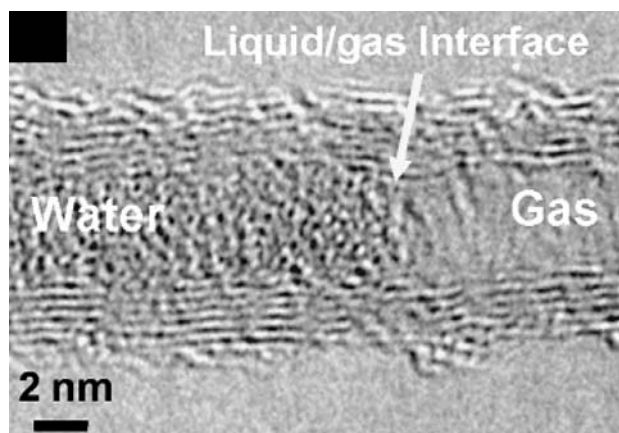
Fig. 12 TEM image of a water-filled (autoclave treated), 4 nm inner diameter CNT, illustrating the diffuse liquid/gas interface that exists on this confined length scale. Adapted and reprinted with permission from Naguib et al. (2004)

similar to that predicted by molecular dynamics simulations (Bai et al. 2006). Slow liquid dynamics characteristic of ice were suggested, based on the ability to observe these structures in real time within the TEM. The observed water characteristics are perhaps related to the extreme pressures within those small diameter hydrothermal nanotubes and potentially the presence of the aforementioned surface functionalities on the tube inner walls. Conversely, under

ambient conditions with open-ended CNTs, water may adopt a very different structure and the experimental measurements with CNT membranes (Majumder et al. 2005; Holt et al. 2006) have suggested relatively fast dynamics for water.

These in situ TEM measurements give a fascinating glimpse into the behavior of fluids within nanotubes, and on the nanometer length scale allow direct visualization of static structures that water adopts with video frame rate resolution (∼60 Hz). However, for visualization of fast, dynamic processes of water within nanotubes, as might occur in open-ended CNTs under near-ambient conditions, time resolution better than video frame rate is needed. The recent developments in dynamic transmission electron microscopy (DTEM; King et al. 2005), which combines the high spatial resolution of conventional TEM with nanosecond time resolution created by use of laser-driven photoemission, may open the door to studying such fast nanofluidic phenomena.

2.2.3 Ultrafast electron diffraction (UED)

Another powerful high spatial and temporal resolution technique is ultrafast electron diffraction (UED), a method that enables electron diffraction patterns to be obtained on samples with time resolution sufficiently fast to probe changes in atomic configuration. The pioneering work in this area, applied to the study of gas phase chemical reactions, was carried out by Zewail et al. (Srinivasan et al. 2003). This technique is advantageous to X-ray-based methods because electrons are scattered not only by the electron distribution in the constituent atoms of the sample, but also by the atomic nuclei. Because of Coulombic scattering effects, the electron-scattering cross section is approximately 6 orders of magnitude higher than the X-ray-scattering cross section of molecules (Hargittai 1988), meaning that the time required to obtain sufficiently bright diffraction patterns from a sample is dramatically reduced. The third generation version of a UED apparatus developed in Zewail's laboratory is capable of a spatial resolution of 0.01 Å and time resolution of 1 ps, suitable for the imaging of transient molecular structures.

Relevant to our discussions here on nanofluidics is the application of UED to study the structure and dynamics of interfacial water. One report (Ruan et al. 2004a) details structural changes induced in a thin epitaxial layer of ice on a hydrophilic (chlorine-coated) silicon (111) substrate, following short pulse (120 fs) infrared laser heating. The disruption of the long-range order in the ice layer induced by laser heating was approximately 10 times slower than in bulk liquid water and similar to the time scales for melting near hydrophilic protein surfaces. Figure 13 shows time lapsed differences in the radial distribution functions (derived from corresponding electron diffraction images) for this ice layer, prior to and following laser heating, along with an illustration of the corresponding changes in water structure that accompany the heating process. Interestingly, they also report (Ruan et al. 2004b) that interfacial ordering of water molecules is different with a hydrogen terminated hydrophobic silicon surface possessing (110) orientation, and absent altogether on a silver-coated, hydrophobic surface. Such results on the behavior of interfacial water are potentially relevant to the study of water structure and transport within nanometer scale hydrophilic (e.g., silica; Fan et al. 2003) and hydrophobic tubules (e.g., CNTs; Majumder et al. 2005; Holt et al. 2006)

### 2.2.4 Nuclear magnetic resonance (NMR)

NMR is a powerful technique commonly used to aid structural determination of organic compounds. The technique is also useful in studying water structure and dynamics at the nanoscale. Protons in hydrogen bonded liquids, like water, interact with one another through what is termed spin–spin coupling (Atkitt and Mann 2000). The relaxation times associated with this spin–spin coupling vary greatly between water (∼seconds) and ice (∼microseconds) and this provides a means by which non-frozen confined water[2] and frozen bulk water in a given sample may be distinguished (Ghosh et al. 2004).

However, in comparison to some of the other techniques that have been presented, the accessible time scales are somewhat longer, several ns, as dictated by the magnetic field frequency. This means that the results obtained are time-averaged over many vibrational periods of water molecules. It is also worth noting that chemical shifts, indicative of the local electronic environment of the protons in an NMR spectrum, are influenced by a number of effects. Oftentimes this means a peak must be deconvoluted into its constituent components to obtain useful structural information, which can be complicated (Ohtaki and Radnai 1993).

With these limitations in mind, however, it is worth highlighting several studies that have used the technique to probe water in CNTs. ^{1}H NMR was recently used to study freezing transitions of water adsorbed by SWCNTs (Ghosh et al. 2004). A downfield feature in the spectrum persisted to temperatures as low as 217 K, and was assigned to water inside the tubes. Another series of studies examined ^{1}H and ^{2}H peak line width in water adsorbed by SWCNTs, indicative of the relative mobility of water, as a function of

---

[2] As a reminder, the aforementioned neutron scattering study indicated that water in CNTs retains fluidity down to 50 K because of a confinement-induced reduction in the number of hydrogen bonds per water molecule. (Kolesnikov et al. 2004)
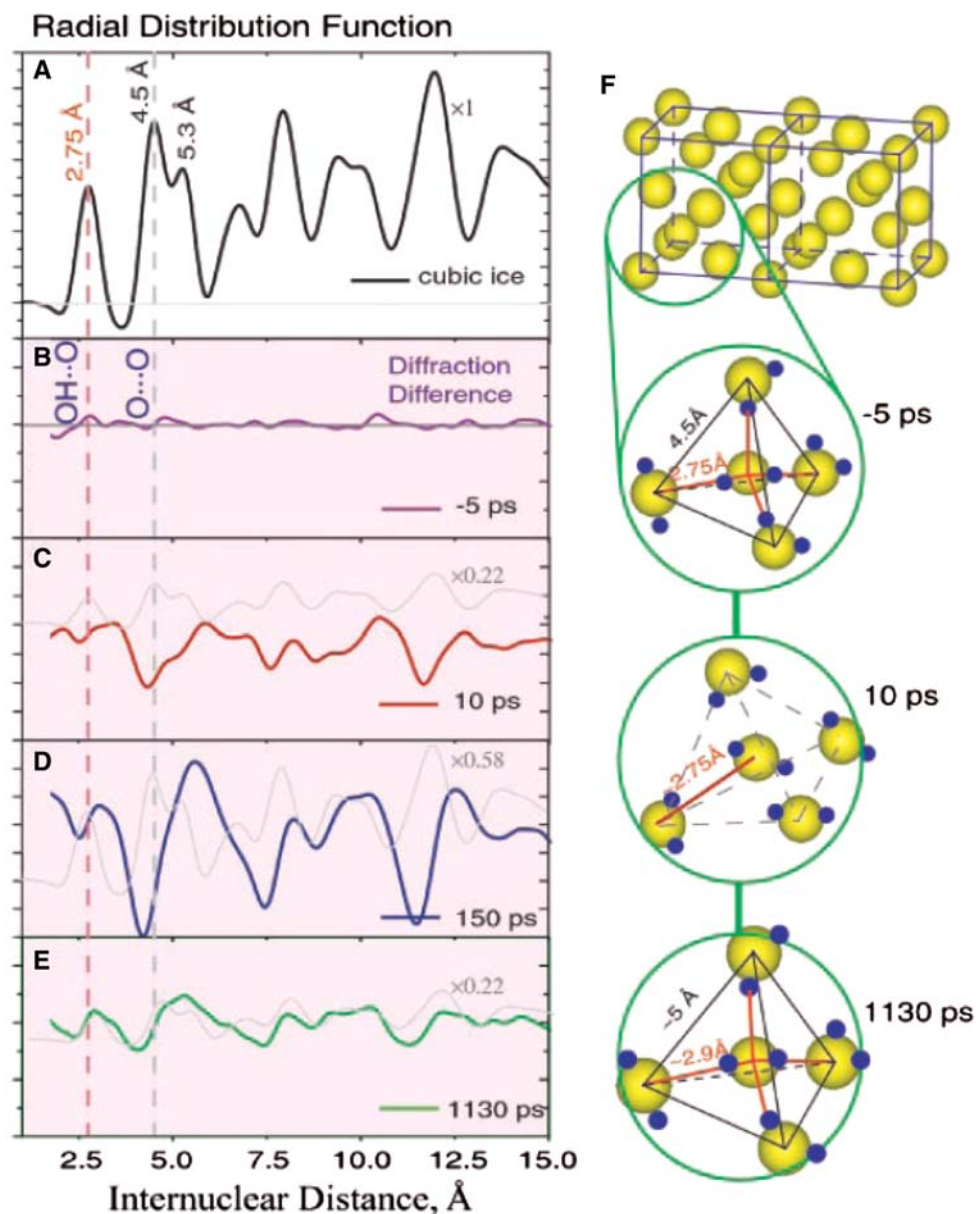
temperature (Matsuda et al. 2006). Figure 14 shows the ^{2}H NMR spectra as a function of temperature. A single sharp line is observed at high temperature, with broadening observed at lower temperatures, giving rise to a double peaked fine structure component. This fine structure is believed to arise from water molecules having different rotational motions. The explanation offered for this phenomenon is the anisotropy in water rotational motion because of orientational effects induced by water-adsorbent and water–water interactions (Matsuda et al. 2006). ^{1}H NMR is also useful in determining water adsorption isotherms, given that peak areas are proportional to proton concentrations. Provided that appropriate standards and calibrations are run, the amount of water in each distinct (chemical shifted) environment can be determined. One study (Mao

et al. 2006) demonstrated that for SWCNTs having a high defect density, water resides principally near the ends of the tubes, rather than filling the entire tube volume. This result is potentially relevant to the intended nanofluidic applications of CNTs, where control of the defect density may be key to achieving significant water occupancy and fast flow through the channels. Nevertheless, low spectral resolution often makes it difficult to separate different species of water that have subtly different electronic environments (e.g., water near the inner and outer walls of a CNT). To address this problem, another study (Sekhaneh et al. 2006) utilized magic angle spinning (MAS) ^{1}H NMR to increase spectral resolution. The two closely spaced peaks (1.2 ppm apart) observed in the spectra of water adsorbed by SWCNTs were assigned to water interior and exterior to the nanotubes.
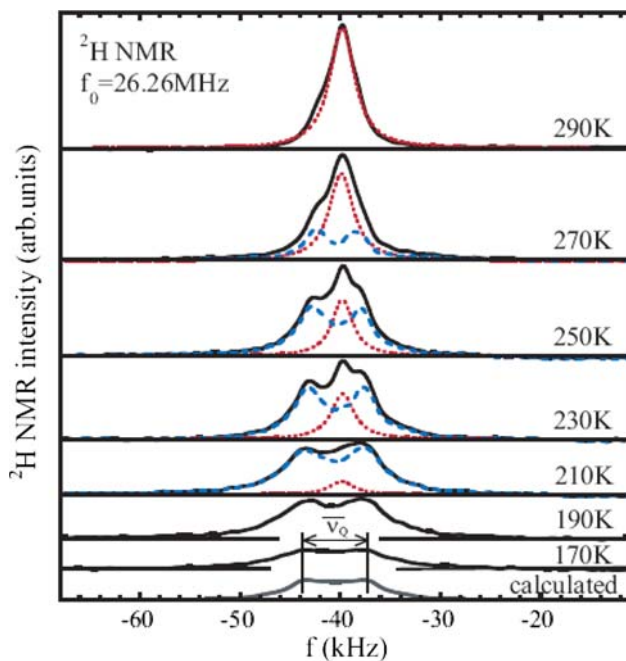
Fig. 14 Temperature dependence of the deuterium NMR spectra. *Red* indicates the single-peak (Lorentzian) and *blue* indicates the double-peaked components to a given spectrum. At low temperatures, fine structures are observed, ascribed to water molecules having different rotational motions. Reprinted with permission of Matsuda et al. (2006)

Another variant of standard NMR is the pulsed field gradient (PFG) technique (Stejskal and Tanner 1965), which is particularly useful in probing dynamic properties of water molecules. The technique can cover a range of diffusion coefficients from 10^{-4} to 10^{-10} cm^2/s, within the range of most types of molecular diffusion. Specifically, PFG NMR can determine the self diffusion coefficient, which is diffusion in the absence of a chemical potential gradient and reveals information on molecular organization and structural changes and, as such, is useful in probing restricted molecular motion (Wu 1991). An early study (Parravano et al. 1967) utilized the technique to study water diffusion in a nanoporous aluminosilicate (zeolite) having pores of 1.2 nm in diameter with the principal finding that water diffusion was comparable to that of free or bulk water. The method is also useful in probing the pore architecture of nanoporous materials, providing information that conventional techniques such as X-ray diffraction often cannot. One study in particular (Stallmach et al. 2000) utilized another nanoporous (~ 3 nm diameter) silica material (MCM-41), demonstrating that diffusion was highly anisotropic. These results suggested two possibilities: (1) in addition to diffusion along the channel, diffusion through the pore walls was occurring, or (2) there was some bending of the pore channels over the probed diffusion length scale. Such results highlight the strength of this technique as a unique probe of molecular diffusion processes on the nanometer scale.

3 Modeling techniques

The experimental techniques presented provide a detailed glimpse of the microscopic properties of water (e.g., hydrogen bond breaking/forming), which often show deviations from bulk properties under nanoscale confinement. These changes in water properties can in turn have significant implications for the collective flow of water molecules through a nanofluidic channel. On the nanometer scale, continuum concepts such as a velocity profile or fluid viscosity may be difficult to define, and for this reason, researchers frequently resort to molecular dynamics (MD) simulations to describe fluid flow. These simulations are often needed to characterize the noncontinuum behavior of fluids that occurs with phenomena such as slip flow (a finite fluid velocity at the channel wall) or high shear stresses. However, the difficulty in producing an accurate water model, as well as the computational expense associated with MD simulations, has prompted researchers to investigate the use of continuum mechanical models that ordinarily operate on the meso- or macroscale for nanoscale flow. If the noncontinuum fluid behavior is captured by molecular modeling, then a realistic boundary condition can be determined and used with continuum hydrodynamic equations to "sweep the molecular details under the rug" (Koplik and Banavar 1995). Such methods are referred to as "hybrid" MD/continuum simulations.

3.1 Continuum mechanical modeling

Continuum mechanical modeling was recently used to describe nanoscale flow within a CNT (Yang 2007). In this study, the fluid inside of a CNT channel was treated as an Eyring fluid, in which the viscosity is shear stress dependent, and produces the phenomenon of shear thinning. This model is in contrast to Newtonian fluids, in which the viscosity is shear stress independent. The Eyring fluid model is appealing in the sense that it is not a phenomenological or empirical model, but has a sound theoretical basis, based on a thermally activated, stress-aided mechanism for viscous flow (Persson 2000). However, the model requires molecular interaction in the direction normal to the shear plane, and may be an imperfect description of fluid flow through nanotubes that may be only a few molecules in diameter. Indeed, it was found that the experimentally observed orders of magnitude enhancements.[3] in water flow through CNTs (Majumder et al. 2005; Holt et al. 2006) could only be reproduced by the Eyring fluid model with the introduction of a slip length. This slip length was

---

[3] The enhancement is measured relative to predictions of no-slip, hydrodynamic flow through a cylindrical channel, i.e., Hagen-Poiseuille flow.

comparable to the nanotube radius and applied to conditions of moderate pressure gradients. The experimental measurements of fluid flow through CNTs (Majumder et al. 2005; Holt et al. 2006) suggest slip lengths many orders of magnitude larger than the nanotube channel, although treating the fluid as Newtonian in this case. On this basis, it is concluded that the Eyring model can be used to treat flow in nanotubes in a continuum mechanics fashion.

What can be concluded from these results? Certainly the validity of the continuum approximation should be carefully examined when trying to describe fluid flow through a channel of molecular dimensions. Provided it is valid within a certain range of parameters, the particular fluid model used must also be carefully examined. It may indeed be the case that fluids that behave as Newtonian on the macroscale (e.g., water) may exhibit significant deviations from that behavior on the nanoscale.

3.2 Molecular modeling

One of the central issues to molecular modeling of water is the development of an accurate potential to describe molecular interactions. As noted in a review of molecular modeling of water (Guillot 2002), researchers have carried out computer simulations of water for three decades, with the goal accurately reproducing its properties over a range of thermodynamic conditions. Such efforts have led to the development of more than 40 such water models, indicative of the importance of this problem, but also highlighting the limited range of applicability of any one model. This outcome is perhaps not surprising, considering that the models are typically developed with the goal of producing a good fit for just one water parameter (e.g., critical point parameters). Attempts to apply any one model to a wider range of water environments frequently result in discrepancies with experiments. An important question for the field of nanofluidics, and relevant for this review, is whether molecular models can accurately predict the properties of water on the nanometer scale. Efforts to answer that question are still ongoing, as the work on simulations has outpaced experiments, particularly concerning transport through nanotubes. As with some of the earlier experimental examples, the focus of this section will be on simulations of water flow through CNTs and highlights of some of the predictions made, rather than a debate on the relative merits of the potentials used, which await experimental validation.

One molecular dynamics (MD) study (Gordillo and Marti 2000) that investigated water structure within CNTs found that the average number of hydrogen bonds decreases when compared with bulk water for tubes ranging in size from 0.8 to 1.6 nm in diameter. Hummer et al. have conducted a number of MD simulations of water confined within CNTs,

with the earliest predicting one-dimensional ordering of water molecules within 0.8 nm CNTs, leading to a concerted, pulse-like movement of the molecules through the channel due to the tight hydrogen bonding network (Hummer et al. 2001). This mechanism is analogous to that seen in zeolites, ion channels and aquaporins (Berezhkovskii and Hummer 2002). It is noteworthy, however, that the thermodynamics and kinetics of channel filling were found to be highly sensitive to the tube wall/water interaction potential (Waghe et al. 2002), which mimics changes in solvent characteristics. This group later examined osmotically driven transport of water through a model 0.8 nm SWCNT membrane (Kalra et al. 2003), finding transport rates of six molecules per ns, on par with those through aquaporin channels (Fig. 15); the flow was found to be semi-frictionless and nearly independent of channel length, in stark contrast to macroscopic flow. Interestingly, the corresponding water flux is comparable to that later measured experimentally, normalizing for differences in tube diameter and driving force (Holt et al. 2006). Another active area of study concerns novel phase transitions of water within CNTs, with the earliest of these studies revealing the formation of intriguing ice phases consisting of hexagonal and
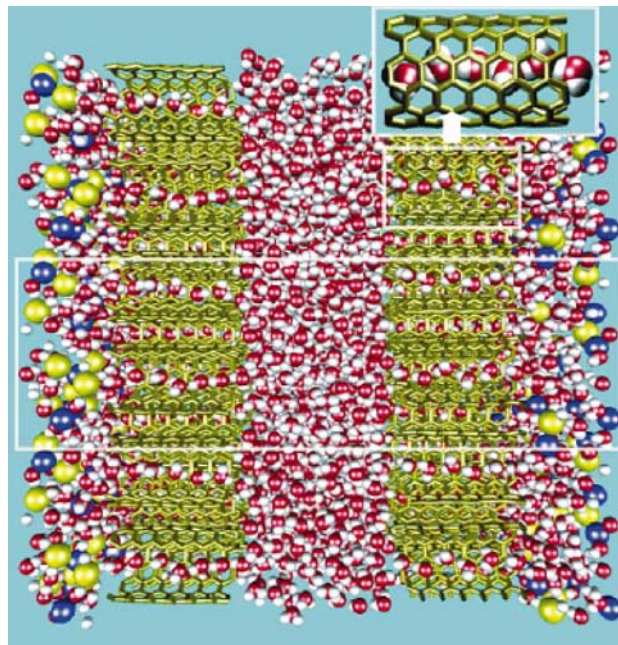

Fig. 15 An MD simulation of water transport through a hexagonally packed array of 0.8 nm diameter SWCNTs. *Blue* denotes Na^+, *yellow* Cl^-, *red* O and *white* H. Owing to the sub-nm pores, only water can flow through the CNTs and it adopts a single file structure. The inner compartment contains pure water, while the exterior contains NaCl at an initial concentration of 5.8 M. Due to the resulting osmotic pressure difference, water drains from the central compartment at a relatively fast rate of ~ 6 molecues per ns per nanotube. Reprinted with permission from Kalra et al. (2003). Copyright (2003) National Academy of Sciences, USA

Fig. 16 *Side* and *top* view of a model system used to probe water gating through an SWCNT; the SWCNT is embedded in a graphite sheet, with a mobile charge (value of +1.0 e) moving in the plane of the graphite. δ indicates the distance between this mobile charge and the CNT surface. *Right*: the dependence of water flow/flux on δ. Adapted and reprinted with permission from Li et al. (2007). Copyright (2007) National Academy of Sciences, USA
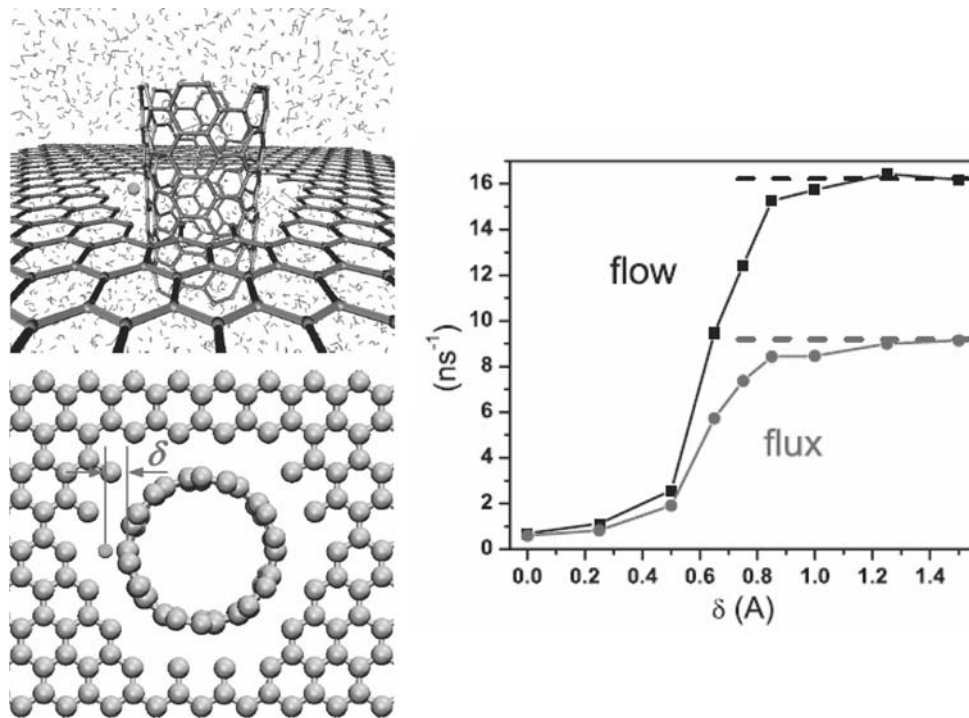
heptagonal ice nanotubes, albeit at relatively large applied axial pressures of 50–500 MPa (Koga et al. 2001). A later study (Shiomi et al. 2007) investigated the diameter dependence of this phase change process, suggesting that these transitions can actually occur under ambient conditions, similar to observations of earlier X-ray diffraction studies (Maniwa et al. 2005).

The structure that water adopts within a CNT can also have implications for the transport of protons. First principles MD simulations (Mann and Halls 2003) found, as with previous studies, that water within a 0.8 nm SWCNT forms a tightly bound, one-dimensional wire and produces a net dipole moment along the nanotube axis. Furthermore, it was predicted that an excess proton injected into the wire forms a stabilized $H_9O_4^+$ complex that effectively traps the proton inside the CNT. However, with the application of an electric field along the tube axis, the proton is conducted through the tube in a manner similar to that in biological channels. A later study (Dellago and Hummer 2006) suggested that protons move diffusively along the water chains and that the passage through the membrane is opposed by a barrier that reflects the energy penalty associated with proton desolvation; the net result is a proton transport rate of 1 per hour per tube under neutral pH conditions.

Another study (Li et al. 2007) suggests that it is possible to gate water transport through a CNT with the inclusion of a single mobile external charge. The position of this charge relative to the CNT wall (with a critical distance of ~ 0.9Å) dictates the on–off behavior of the channel to

water permeation, with a more than one order of magnitude difference in flow, depending on this distance (Fig. 16). Water transport has also been found to be sensitive to relative hydrophobicity of the CNT wall. A recent study examined this effect by modifying the Lennard-Jones parameters of the CNT wall, having it span from a hydrophobic CNT to the relatively hydrophilic silicon (Joseph and Aluru 2008). The CNT flow enhancement is greatly reduced with the hydrophilic surface, due to OH bond reorientation and increased hydrogen bonding. The effect of roughness was also modeled by joining two different diameter CNTs, with virtually no flow enhancement observed in these channels. These studies attempt to capture some of the non-idealities that experimentalists encounter when working with imperfect CNTs (i.e., those containing defects), highlighting the need for high-quality CNTs to utilize their unique properties. These studies also highlight some of subtleties that both proton and water transport depend on and shed light on mechanisms that enable exquisite selectivity in biological systems, amidst an often chaotic, thermally fluctuating environment. Insights gained into these mechanisms can potentially be exploited for applications in, for example, proton exchange fuel cell membranes, where control of water and proton transport is critical.

Other molecular simulations attempt to study flow structure within the CNTs. One study (Kotsalis et al. 2004) describes a nonequilibrium MD simulation of the steady-state Poiseuille-like flow of water as well as water/nitrogen

mixtures through CNTs with diameters ranging from 3 to 5 nm; a constant flow rate is fixed in the system through the use of what is termed an "adaptive forcing scheme". For pure liquid transport, confinement is found to induce layering of molecules near the CNT wall. As an example, Fig. 17 shows MD simulation snapshots of water transport at 300 and 500 K. The layering evident at 300 K is virtually nonexistent at 500 K. Also, in the case of transport of a liquid/vapor mixture, this layering was absent. In the case for which "nanobubbles" were introduced into the system, it was believed that shielding of the bulk flow from the CNT surface occurred due to the creation of a liquid/vapor interface. These results have potentially significant implications for real applications of CNT nanofluidics, where

Fig. 17 MD simulation snapshots of water flow through a 2.7 nm diameter CNT at 300 K (*top*) and at 500 K (*bottom*). Variations in density and layering of water molecules are evident at 300 K that are not present at 500 K. Reprinted with permission of Kotsalis et al. (2004)

elevated temperatures and dissolved gases that affect water structure may in turn alter water dynamics. Another recent study (Hanasaki and Nakatani 2006) addresses the question of whether water flow through CNTs (0.8–3 nm in diameter) can truly be described as Poiseuille- or plug-like. Water is driven through the CNTs in these MD simulations through the use of "fluidized piston" and "ice piston" models. In the smallest CNTs considered, water flow occurs in a single-file manner, with a convex upward streaming velocity profile, caused by friction between the fluid molecules and the atoms of the wall. For the larger CNTs considered, streaming velocity profiles are flat, with the exception of the near-wall region. On this basis, they conclude that water flow is more plug-like than Poiseuille-like in CNTs, although it is not strictly accurate to describe the flow as either.
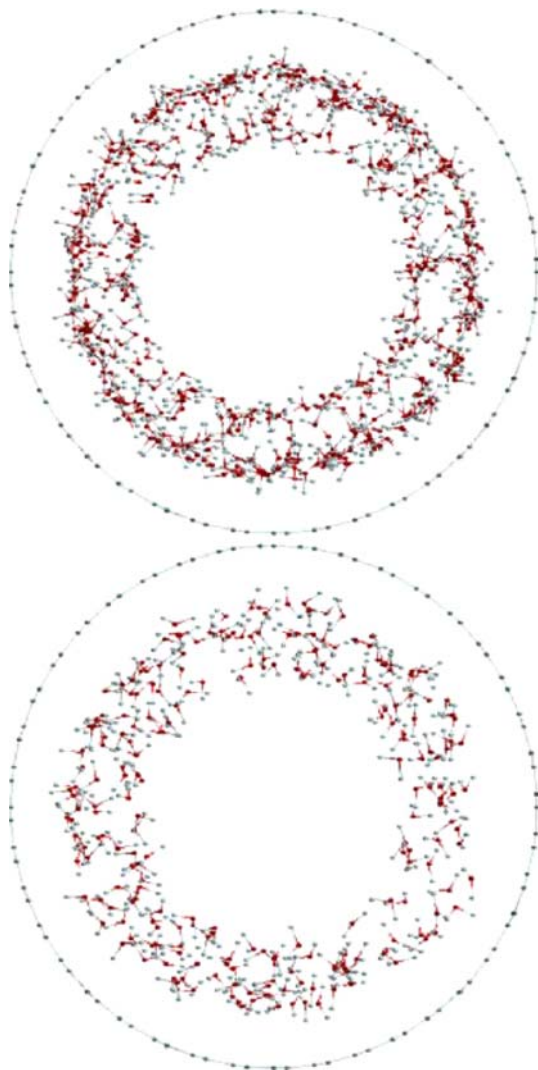
3.3 Hybrid methods

Finally, it is worth pointing to another category of simulation that is a combination of molecular dynamics and continuum-type models, referred to as a hybrid model. The idea behind this method is to characterize the near-wall flow regions atomistically with MD, while the core region is characterized by a continuum model (i.e., Navier-Stokes equation). Such an approach reduces the computational burden associated with characterizing mesoscale flow that occurs on the slightly larger length scales of 10–100 nm. An example of such a hybrid method was recently described (Yen et al. 2007), where it was applied to the study of Couette and Poiseuille flows (with interfacial slippage) having channel dimensions on the nano- and mesoscale. The principal finding was that the near-wall MD region must be at least 12 molecular diameters in size, with an overlap region (between the MD and continuum regions) of at least 10 molecular diameters. Although these are larger length scales where molecular confinement effects may be absent, they are potentially relevant for next generation lab-on-a-chip applications, and for which adequate simulation methods are needed.

3.4 Modeling summary

It should be clear from these examples that there is a large body of simulation results on flow through CNTs, utilizing a host of different methods that attempt to cover the sub-nm to 100 nm length scales. What is lacking is a comparable amount of experimental nanofluidics results. However, with a host of new studies utilizing both established (e.g., PFG-NMR) and novel techniques (e.g., direct flow measurement through nanotube arrays), there is a growing body of data to which such simulations can be compared and subsequently validated or refuted.

4 Summary and perspectives

A variety of different experimental and modeling techniques have been presented, some of which have been traditionally used to study the properties of bulk water. Many of these techniques have a sufficiently high resolution (spatially and temporally) that render them useful for studying water under nanoscale confinement. The various spectroscopy, scattering, microscopy and modeling techniques discussed lend extremely useful insights into water structure and dynamics on length and time scales relevant to nanofluidics.

An obvious question that emerges is whether some of the results discussed contradict one another, reflecting experimental errors and errors in analysis, or are the observed differences merely a reflection of the different time scales being probed? Is the "static picture" of water (Zubavicus and Grunze 2004) derived from the diffraction/scattering techniques, consisting of an interconnected, tetrahedral hydrogen bridge bond network, consistent with the results obtained from ultrafast techniques? Results from the ultrafast techniques presented suggest novel water structures (e.g., rings, chains) that scattering measurements reveal cannot be persistent over long length scales. However, would time averaging of ultrafast data allow one to reproduce the equilibrium distribution within a network of water molecules and provide results consistent with those obtained from diffraction? These are questions that researchers will need to tackle in the coming years.

It is clear that there is no "silver bullet" when it comes to determining an accurate picture of water structure and dynamics. Any given experimental technique will have its own limited range of applicability (i.e., time, length scales), and that should be kept in mind when interpreting what might otherwise appear to be contradictory results obtained by different techniques. One must also evaluate models in a similar way; they often only provide a description of water within a very limited range of thermodynamic parameters. However, as with the study of numerous other systems, experiments and simulations are complementary. Simulations are often uncovering unique phenomena that motivate experimentalists to pursue their study. Indeed, MD simulations of water confinement in CNTs (Hummer et al. 2001; Kalra et al. 2003; Dellago and Hummer 2006) provided the impetus to develop CNT membranes (Hinds et al. 2004; Holt et al. 2004, 2006; Majumder et al. 2005) to test predictions of flow enhancement. Similarly, experiments provide the details of water molecule interactions with one another and provide useful input to theoreticians who attempt to produce ever more accurate water potentials.

With this toolbox of experimental and simulation techniques at our disposal, and the ability to make direct comparisons between the two, the future remains promising as researchers continue to unravel the structure and dynamics of water in nanoscale systems.

References

Agmon N (1995) The Grotthuss mechanism. Chem Phys Lett 244:456–462

Agre P, MacKinnon R (2003) Information for the public. The Nobel Prize in Chemistry 2003, © The Nobel Foundation

Agre P (2004) Aquaporin water channels (Nobel lecture). Angewandte Chemie (international edition) 43:4278–4290

Atkitt JW, Mann BE (2000) NMR and chemistry: an introduction to modern NMR spectroscopy. CRC Press, West Palm Beach

Bai JE, Wang J, Zeng XC (2006) Multiwalled ice helixes and ice nanotubes. Proc Nat Acad Sci USA 103:19664–19667

Berezhkovskii A, Hummer G (2002) Single-file transport of water molecules through a carbon nanotube. Phys Rev Lett 89:064503

Bergmann U, Wernet P, Glatzel P, Cavalleri M, Pettersson LGM, Nilsson A, Cramer SP (2002) X-ray Raman spectroscopy at the oxygen K edge of water and ice: implications on local structure models. Phys Rev B 66:092107

Chen J, Hamon MA, Hu H, Chen YS, Rao AM, Eklund PC, Haddon RC (1998) Solution properties of single-walled carbon nanotubes. Science 282:95–98

Cowan ML, Bruner BD, Huse N, Dwyer JR, Chugh B, Nibbering ETJ, Elsaesser T, Miller RJD (2005) Ultrafast memory loss and energy redistribution in the hydrogen bond network of liquid H$_2$O. Nature 434:199–202

Dellago C, Hummer G (2006) Kinetics and mechanism of proton transport across membrane nanopores. Phys Rev Lett 97:245901

Doyle DA, Cabral JM, Pfuetzner RA, Kuo AL, Gulbis JM, Cohen SL, Chait BT, MacKinnon R (1998) The structure of the potassium channel: molecular basis of K$^+$ conduction and selectivity. Science 280:69–77

Dyke CA, Tour JM (2004) Covalent functionalization of single-walled carbon nanotubes for materials applications. J Phys Chem A 108:11151–11159

Eijkel JCT, van den Berg A (2005) Nanofluidics: what is it and what can we expect from it? Microfluid Nanofluid 1:249–267

Fan R, Wu YY, Li DY, Yue M, Majumdar A, Yang PD (2003) Fabrication of silica nanotube arrays from vertical silicon nanowire templates. J Am Chem Soc 125:5254–5255

Fecko CJ, Eaves JD, Loparo JJ, Tokmakoff A, Geissler PL (2003) Ultrafast hydrogen bond dynamics in the infrared spectroscopy of water. Science 301:1698–1702

Gale GM, Gallot G, Hache F, Lascoux N, Bratos S, Leicknam JC (1999) Femtosecond dynamics of hydrogen bonds in liquid water: a real-time study. Phys Rev Lett 82:1068–1071

Ghosh S, Ramanathan KV, Sood AK (2004) Water at nanoscale confined in single-walled carbon nanotubes studied by NMR. Europhys Lett 65:678–684

Gordillo MC, Marti J (2000) Hydrogen bond structure of liquid water confined in nanotubes. Chem Phys Lett 329:341–345

Guillot B (2002) A reappraisal of what we have learnt during three decades of computer simulations on water. J Mol Liquid 101:219–260

Hanasaki I, Nakatani A (2006) Flow structure of water in carbon nanotubes: Poiseuille type or plug-like? J Chem Phys 124:144708

Hargittai I (1988). Part A: the electron diffraction technique. In: Hargittai I, Hargittai M (eds) Stereochemical applications of gas-phase electron diffraction. VCH, New York

Head-Gordon T, Hura G (2002) Water structure from scattering experiments and simulation. Chem Rev 102:2651–2669

Head-Gordon T, Johnson ME (2006) Tetrahedral structure or chains for liquid water. Proc Natl Acad Sci USA 103:16614–16614

Hinds BJ, Chopra N, Rantell T, Andrews R, Gavalas V, Bachas LG (2004) Aligned multiwalled carbon nanotube membranes. Science 303:62–65

Holt JK, Noy A, Huser T, Eaglesham D, Bakajin O (2004) Fabrication of a carbon nanotube-embedded silicon nitride membrane for studies of nanometer-scale mass transport. Nano Lett 4:2245–2250

Holt JK, Park HG, Wang YM, Stadermann M, Artyukhin AB, Grigoropoulos CP, Noy A, Bakajin O (2006) Fast mass transport through sub-2-nanometer carbon nanotubes. Science 312:1034–1037

Hummer G, Rasaiah JC, Noworyta JP (2001) Water conduction through the hydrophobic channel of a carbon nanotube. Nature 414:188–190

Hura G, Sorenson JM, Glaeser RM, Head-Gordon T (2000) A high-quality X-ray scattering experiment on liquid water at ambient conditions. J Chem Phys 113:9140–9148

Jessel TMK, Eric R, Schwartz, James H. (2000) Principles of neural science. Ion channels, chapter 6. McGraw-Hill, New York, pp 105–124

Joseph S, Aluru NR (2008) Why are carbon nanotubes fast transporters of water? Nano Lett 8:452–458

Kalra A, Garde S, Hummer G (2003) Osmotic water transport through carbon nanotube membranes. Proc Natl Acad Sci USA 100:10175–10180

Karnicky JF, Pings CJ (1976). Recent advances in the study of liquids by X-ray diffraction. In: Prigogine I, Rice SA (eds) Advances in chemical physics. Wiley, New York

King WE, Campbell GH, Frank A, Reed B, Schmerge JF, Siwick BJ, Stuart BC, Weber PM (2005) Ultrafast electron microscopy in materials science, biology, and chemistry. J Appl Phys 97:1–27

Koga K, Gao GT, Tanaka H, Zeng XC (2001) Formation of ordered ice nanotubes inside carbon nanotubes. Nature 412:802–805

Kolesnikov AI, Zanotti JM, Loong CK, Thiyagarajan P, Moravsky AP, Loutfy RO, Burnham CJ (2004) Anomalously soft dynamics of water in a nanotube: a revelation of nanoscale confinement. Phys Rev Lett 93:035503

Koplik J, Banavar JR (1995) Continuum deductions from molecular hydrodynamics. Annu Rev Fluid Mech 27:257–292

Kotsalis EM, Walther JH, Koumoutsakos P (2004) Multiphase water flow inside carbon nanotubes. Int J Multiphase Flow 30:995–1010

Koumoutsakos P, Zimmerli U, Werder T, Walther JH (2004). Nanoscale fluid mechanics, In: Lakhtakia A (ed) Handbook of nanotechnology: nanometer structure theory, modeling, and simulation. ASME Press, New York

Landau EM, Rosenbusch JP (1996) Lipidic cubic phases: a novel concept for the crystallization of membrane proteins. Proc Natl Acad Sci USA 93:14532–14535

Leythaeuser D, Schaefer RG, Yukler A (1980) Diffusion of light hydrocarbons through near-surface rocks. Nature 284:522–525

Li JY, Gong XJ, Lu HJ, Li D, Fang HP, Zhou RH (2007) Electrostatic gating of a nanometer water channel. Proc Natl Acad Sci USA 104:3687–3692

Libera J, Gogotsi Y (2001) Hydrothermal synthesis of graphite tubes using Ni catalyst. Carbon 39:1307–1318

Ludwig R (2001) Water: from clusters to the bulk. Angewandte Chemie (international edition) 40:1808–1827

Majumder M, Chopra N, Andrews R, Hinds BJ (2005) Nanoscale hydrodynamics —enhanced flow in carbon nanotubes. Nature 438:44

Maniwa Y, Kataura H, Abe M, Udaka A, Suzuki S, Achiba Y, Kira H, Matsuda K, Kadowaki H, Okabe Y (2005) Ordered water inside carbon nanotubes: formation of pentagonal to octagonal ice-nanotubes. Chem Phys Lett 401:534–538

Mann DJ, Halls MD (2003) Water alignment and proton conduction inside carbon nanotubes. Phys Rev Lett 90:195503

Mao SH, Kleinhammes A, Wu Y (2006) NMR study of water adsorption in single-walled carbon nanotubes. Chem Phys Lett 421:513–517

Matsuda K, Hibi T, Kadowaki H, Kataura H, Maniwa Y (2006) Water dynamics inside single-wall carbon nanotubes: NMR observations. Phys Rev B 74:073415

Mattia D, Rossi M, Ye H, Gogotsi Y (2007). In situ fluid studies in carbon nanotubes with diameters ranging from 1 to 500 nm. In: 5th IASME/WSEAS international conference on fluid mechanics and aerodynamics, Athens, Greece, pp. 294–296

Morgan J, Warren BE (1938) X-ray analysis of the structure of water. J Chem Phys 6:666–673

Murata K, Mitsuoka K, Hirai T, Walz T, Agre P, Heymann JB, Engel A, Fujiyoshi Y (2000) Structural determinants of water permeation through aquaporin-1. Nature 407:599–605

Myneni S, Luo Y, Naslund LA, Cavalleri M, Ojamae L, Ogasawara H, Pelmenschikov A, Wernet P, Vaterlein P, Heske C, Hussain Z, Pettersson LGM, Nilsson A (2002) Spectroscopic probing of local hydrogen-bonding structures in liquid water. J Phys Condens Matter 14:L213–L219

Naguib N, Ye HH, Gogotsi Y, Yazicioglu AG, Megaridis CM, Yoshimura M (2004) Observation of water confined in nanometer channels of closed carbon nanotubes. Nano Lett 4:2237–2243

Narten AH, Thiessen WE, Blum L (1982) Atom pair distribution-functions of liquid water at 25-degrees-C from neutron diffraction. Science 217:1033–1034

Newville M (2004). Fundamentals of XAFS, Chicago. University of Chicago, Chicago, p. 37

Nilsson A, Wernet P, Nordlund D, Bergmann U, Cavalleri M, Odelius M, Ogasawara H, Naslund LA, Hirsch TK, Glatzel P, Pettersson LGM (2005) Comment on "Energetics of hydrogen bond network: rearrangements in liquid water". Science 308:793A

Ohkubo T, Konishi T, Hattori Y, Kanoh H, Fujikawa T, Kaneko K (2002) Restricted hydration structures of Rb and Br ions confined in slit-shaped carbon nanospace. J Am Chem Soc 124:11860–11861

Ohtaki H, Radnai T (1993) Structure and dynamics of hydrated ions. Chem Rev 93:1157–1204

Page DI (1972). Chapter 9. In: Frank F (ed) Water, a comprehensive treatise. Plenum Press, New York, pp 333–362

Parravano C, Baldeschweiler JD, Boudart M (1967) Diffusion of water in zeolites. Science 155:1535

Persson BNJ (2000) Sliding friction: physical principles and applications. Springer, Heidelberg

Riegelman M, Liu H, Bau HH (2006) Controlled nanoassembly and construction of nanofluidic devices. J Fluid Eng Trans Asme 128:6–13

Ruan CY, Lobastov VA, Vigliotti F, Chen SY, Zewail AH (2004a) Ultrafast electron crystallography of interfacial water. Science 304:80–84

Ruan CY, Lobastov VA, Vigliotti F, Chen SY, Zewail AH (2004b) Unpublished work

Rullmann JAC, Vanduijnen PT (1988) A polarizable water model for calculation of hydration energies. Mol Phys 63:451–475

Sekhaneh W, Kotecha M, Dettlaff-Weglikowska U, Veeman WS (2006) High resolution NMR of water absorbed in single-wall carbon nanotubes. Chem Phys Lett 428:143–147

Shiomi J, Kimura T, Maruyama S (2007) Molecular dynamics of ice-nanotube formation inside carbon nanotubes. J Phys Chem C 111:12188–12193

Smith JD, Cappa CD, Wilson KR, Messer BM, Cohen RC, Saykally RJ (2004) Energetics of hydrogen bond network rearrangements in liquid water. Science 306:851–853

Smith JD, Cappa CD, Messer BM, Cohen RC, Saykally RJ (2005a) Response to comment on "Energetics of hydrogen bond network: rearrangements in liquid water". Science 308:793B

Smith JD, Cappa CD, Wilson KR, Cohen RC, Geissler PL, Saykally RJ (2005b) Unified description of temperature-dependent hydrogen-bond rearrangements in liquid water. Proc Natl Acad Sci USA 102:14171–14174

Soper AK, Bruni F, Ricci MA (1997) Site–site pair correlation functions of water from 25 to 400 degrees C: revised analysis of new and old diffraction data. J Chem Phys 106:247–254

Soper AK (2000) The radial distribution functions of water and ice from 220 to 673 K and at pressures up to 400 MPa. Chem Phys 258:121–137

Sprik M, Klein ML (1988) A polarizable model for water using distributed charge sites. J Chem Phys 89:7556–7560

Srinivasan R, Lobastov VA, Ruan CY, Zewail AH (2003) Ultrafast electron diffraction (UED)—a new development for the 4D determination of transient molecular structures. Helvetica Chimica Acta 86:1763–1838

Stallmach F, Karger J, Krause C, Jeschke M, Oberhagemann U (2000) Evidence of anisotropic self-diffusion of guest molecules in nanoporous materials of MCM-41 type. J Am Chem Soc 122:9237–9242

Stejskal EO, Tanner JE (1965) Spin diffusion measurements—spin echoes in presence of a time-dependent field gradient. J Chem Phys 42:288

Stillinger FH (1980) Water revisited. Science 209:451–457

Tohji K, Udagawa Y (1989) X-ray Raman-scattering as a substitute for soft-X-ray extended X-ray absorption fine structure. Phys Rev B 39:7590–7594

Tokmakoff A (2007) Shining light on the rapidly evolving structure of water. Science 317:54–55

Waghe A, Rasaiah JC, Hummer G (2002) Filling and emptying kinetics of carbon nanotubes in water. J Chem Phys 117:10789–10795

Wallen SL, Palmer BJ, Pfund DM, Fulton JL, Newville M, Ma YJ, Stern EA (1997) Hydration of bromide ion in supercritical water: an X-ray absorption fine structure and molecular dynamics study. J Phys Chem A 101:9632–9640

Wernet P, Nordlund D, Bergmann U, Cavalleri M, Odelius M, Ogasawara H, Naslund LA, Hirsch TK, Ojamae L, Glatzel P, Pettersson LGM, Nilsson A (2004) The structure of the first coordination shell in liquid water. Science 304:995–999

Wu S (1991). Pulsed field gradient nuclear magnetic resonance and applications in Y type zeolites, University of Nebraska

Yang FQ (2007) Flow behavior of an Eyring fluid in a nanotube: the effect of the slip boundary condition. Appl Phys Lett 90:133105

Yazicioglu AG, Megaridis CM, Nicholls A, Gogotsi Y (2005) Electron microscope visualization of multiphase fluids contained in closed carbon nanotubes. J Vis 8:137–144

Ye H, Naguib N, Gogotsi Y (2004) TEM study of water in carbon nanotubes. JEOL News 39:38–43

Yen TH, Soong CY, Tzeng PY (2007) Hybrid molecular dynamics-continuum simulation for nano/mesoscale channel flows. Microfluid Nanofluid 3:665–675

Yeremenko S, Pschenichnikov MS, Wiersma DA (2003) Hydrogen-bond dynamics in water explored by heterodyne-detected photon echo. Chem Phys Lett 369:107–113

Zubavicus Y, Grunze M (2004) New insights into the structure of water with ultrafast probes. Science 304:974–976